# Geometry and dynamics of squeezing in finite systems

**Kurt Bernardo Wolf* and Guillermo Krötzsch**

*Instituto de Ciencias Físicas, Universidad Nacional Autónoma de México, Cuernavaca, Morelos 62251, México*
**Corresponding author: bwolf@fis.unam.mx*

Received April 16, 2007; accepted May 23, 2007;
posted May 31, 2007 (Doc. ID 82104); published August 16, 2007

Squeezing and its inverse magnification form a one-parameter group of linear canonical transformations of continuous signals in paraxial optics. We search for corresponding unitary matrices to apply on signal vectors in $N$-point finite Hamiltonian systems. The analysis is extended to the phase space representation by means of Wigner quasi-probability distribution functions on the discrete torus and on the sphere. Together with two previous studies of the fractional Fourier and Fresnel transforms, we complete the finite counterparts of the group of linear canonical transformations. © 2007 Optical Society of America

*OCIS codes:* 070.2590, 070.6020, 070.6760, 080.1010, 090.1970, 200.4560.

## 1. INTRODUCTION: CLASSICAL SQUEEZING

In the continuous models of paraxial optics and quadratic potentials in quantum mechanics, linear canonical transformations form a privileged three-parameter Lie group, which may be represented by $2\times 2$ real matrices of unit determinant. The Iwasawa decomposition of this group is

$$\begin{bmatrix} a & b \\ c & d \end{bmatrix} = \begin{bmatrix} \cos\omega & -\sin\omega \\ \sin\omega & \cos\omega \end{bmatrix} \begin{bmatrix} e^{\alpha} & 0 \\ 0 & e^{-\alpha} \end{bmatrix} \begin{bmatrix} 1 & 0 \\ z & 1 \end{bmatrix}. \tag{1}$$

Acting on the phase space vector $\binom{p}{q}$ of position $q$ and momentum (paraxial ray inclination) $p$, the left-hand term of Eq. (1) represents a fractional Fourier transform, while the right-hand term yields free-wave propagation by a Fresnel transform. The finite counterparts of these two transforms have been analyzed in [1,2], respectively. We now address the middle factor, squeezing (or magnification), which shrinks (or expands) positions $q\mapsto e^{-\alpha}q$, and momenta $p\mapsto e^{\alpha}p$, with $\alpha\in\mathsf{R}$. These transformations form the one-parameter group of scalings; we use the term "squeezing" as in quantum optics, or "magnification" as is common in geometric and wave optics, because finite systems are purported to abstract both theories.

*Prima facie* it would seem that on finite $N$-point signals, where the position coordinate of the sensors takes a finite number of fixed discrete values, squeezing or magnification by arbitrary real factors cannot be performed without losing information. The same applies to two-dimensional pixellated images. As we shall see, however, we may treat squeezings as *aberrations* of an appropriate phase space and represent them by $N\times N$ unitary matrices. As we did in [1,2], we shall consider two distinct models for finite systems: periodic systems, where the transformation between position and momentum is the discrete Fourier transform (DFT) matrix, and nonperiodic systems, where this role is taken by the Fourier–Kravchuk transform (FKT), which is a rotation by $\frac{1}{2}\pi$ in the familiar group $\mathsf{SU}(2)$ of quantum angular momentum theory. Each of these two models has a corresponding phase space; in the periodic case it is the discrete torus $(m,k)$ of integers modulo $N$, while for the $\mathsf{SU}(2)$ case it is essentially the 2-sphere.

In the classical Hamiltonian models of optics and mechanics, where the basic Poisson bracket between position and momentum is $\{q,p\}_{\mathrm{Pb}}=1$, squeezing is generated by the Lie exponential of the Poisson-bracket operator of the monomial $qp$,

$$S(\alpha):f(q,p) := \exp(\alpha\{qp,\circ\}_{\mathrm{Pb}}):f(q,p) = f(e^{-\alpha}q,e^{\alpha}p). \tag{2}$$

This produces a flow of phase space $(q,p)\in\mathsf{R}^2$ along the hyperbolas $qp=$constant, as shown in Fig. 1. Similarly, free Fresnel propagation, fractional Fourier, and Fresnel-lens (chirp) transforms are generated by the quadratic functions of $(q,p)$,

$$g_{\mathrm{Fr}} := \frac{1}{2}p^2, \qquad g_{\mathrm{Fou}} := \frac{1}{2}(p^2+q^2), \qquad g_{\mathrm{FL}} := \frac{1}{2}q^2, \tag{3}$$

respectively. The generator of squeezing [Eq. (2)] can be obtained either through direct multiplication of $q$ and $p$ or through a Poisson bracket of Eq. (3) as

$$g_{\mathrm{S}}(q,p) = qp = \{g_{\mathrm{FL}},g_{\mathrm{Fr}}\}_{\mathrm{Pb}}. \tag{4}$$

In wave models, such as Fourier optics and quadratic quantum mechanics, $q$ and $p$ are replaced by the Schrödinger operators $\mathcal{Q}:f(q)=qf(q)$ and $\mathcal{P}:f(q)=-\mathrm{i}\mathrm{d}f(q)/\mathrm{d}q$, which are essentially self-adjoint on the Hilbert space of square-integrable wave functions $f(q)\in\mathcal{L}^2(\mathsf{R})$, and satisfy the Heisenberg commutator $[\mathcal{Q},\mathcal{P}]=\mathrm{i}I$. Here, squeezing is generated by the Lie exponential of the Weyl-ordered operator that corresponds to $qp$,

$$\mathcal{S}(\alpha):f(q) := \exp(\mathrm{i}\alpha\{\mathcal{Q}\mathcal{P}\}_{\mathrm{W}}):f(q) = e^{-\alpha/2}f(e^{\alpha}q), \tag{5}$$

where

 

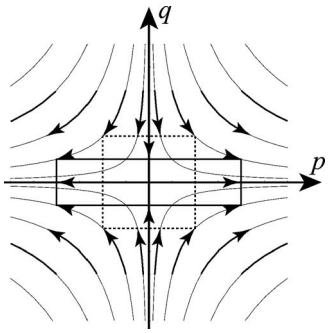


Fig. 1. Squeezing $S(\alpha)$ classically produces a flow of phase space $(q,p)\in\mathsf{R}^2$ along the hyperbolas $qp=\text{const}$. For $\alpha>0$, positions are squeezed, momenta (wavenumbers) are magnified, and areas are conserved.

$$\{\mathcal{QP}\}_{\mathrm{W}} := \frac{1}{2}(\mathcal{QP}+\mathcal{PQ}) = -\mathrm{i}q\frac{\mathrm{d}}{\mathrm{d}q} - \mathrm{i}\frac{1}{2}\mathit{1} = -\mathrm{i}\left[\frac{1}{2}\mathcal{Q}^2,\frac{1}{2}\mathcal{P}^2\right]. \tag{6}$$

For quadratic functions such as Eqs. (3) and (4), the correspondence between classical functions with Poisson brackets, and operators with $\mathrm{i}\times$ commutators, is exact. In $\mathcal{L}^2(\mathsf{R})$, the $\mathcal{S}(\alpha)$'s are unitary and form a one-parameter group: $\mathcal{S}(\alpha_1)\mathcal{S}(\alpha_2)=\mathcal{S}(\alpha_1+\alpha_2)$, $\mathcal{S}(0)=1$, and $\mathcal{S}(-\alpha)=(\mathcal{S}(\alpha))^\dagger$, for $\alpha\in\mathsf{R}$. Fresnel and Fourier integral transforms, and chirps, are correspondingly generated by the quantum versions of Eq. (3). Together with squeezing [Eq. (5)], these second-degree differential operators generate the (2:1 cover of the) real symplectic group $\mathsf{Sp}(2,\mathsf{R})$, namely, linear canonical integral transforms [3,4], Chaps. 9 and 10, which are represented by the matrices in Eq. (1).

Can a similar construction be made for finite models? A well-known theorem states that noncompact groups (i.e., groups with infinite invariant volume) do not have finite-dimensional unitary representations [5]; hence, $\mathsf{Sp}(2,\mathsf{R})$ cannot act through $N\times N$ unitary matrices. Yet one needs unitary matrices, elements of the group $\mathsf{U}(N)$, to conserve norms, distances, and angles between complex $N$-point signals. To find the "right" unitary matrices $\mathbf{S}(\alpha)$ for squeezing, we follow the strategy of finding their *generator* matrix, self-adjoint $\mathbf{G}$, using geometrical and/or dynamical arguments. And then the finite squeezing matrices $\mathbf{S}(\alpha)=\exp(\mathrm{i}\alpha\mathbf{G})$ will act directly on the signal $N$-vectors. However, only for *small* values of $\alpha$ can we expect that continuous and finite squeezings will resemble each other. We shall analyze these transformations on phase space rather than only on "how the signals look," because—as we shall see—their Wigner distribution functions [6–8] offer a more penetrating picture of the process.

In Section 2 we look at the possibilities afforded by two standard periodic DFT models, one based on the geometric premise of equally spaced positions, and the other on lattice dynamics with the second-difference matrix, acting on a discrete toroidal phase space. Sections 3 and 4 present the construction based on the group $\mathsf{SU}(2)\subset\mathsf{U}(N)$, where squeezing is generated by a quadratic element in the algebra, which is an aberration of the phase space sphere. In Section 5 we offer some comments and conclusions.

## 2. SQUEEZING ON THE PHASE SPACE TORUS

Since there are no finite $N$-dimensional self-adjoint matrix representations of the Heisenberg algebra, one cannot find exact finite matrix analogs of the classical $\{q,p\}_{\mathrm{Pb}}=1$ nor of the wave/quantum $[\mathcal{Q},\mathcal{P}]=\mathrm{i}\mathit{1}$. What should the finite analog of $qp$ be? We can start with a geometric *ansatz* (g), where the $N\times N$ matrix $\mathbf{Q}^{\mathrm{g}}$ of position is postulated to be diagonal, with distinct and unit-spaced eigenvalues $\lambda^{\mathrm{g}}_m=m\in[-j,j]$, where we write $N=2j+1$. Or, we can propose a dynamical *ansatz* (d) refering to a ring of $N$ equal masses numbered by $m$, joined to first neighbors by equal springs, whose free Hamiltonian is the second-difference matrix [$\mathbf{\Delta}:=\mathrm{circ}(-2,1,0,\ldots,0,1)$, circulating and symmetric] and which is naturally identified with (minus) the square of momentum $(\mathbf{P}^{\mathrm{d}})^2$; in this model the eigenvalues are $\lambda^{\mathrm{d}}_m=4\sin^2(\pi m/N)\in[0,4]$. In both of these finite models—as in continuous Hamiltonian systems—we make the key assumption that the Fourier transform (by the DFT matrix $\mathbf{\Phi}$) of position $m$ is momentum (wavenumber) $k$, with the same spectrum. This matrix transform implies that the states of the system will be periodic in their components $m$ modulo $N$ and that the corresponding phase space is the discrete torus $(m,k)$ modulo $N$.

The $N\times N$ position and $\frac{1}{2}$-square-momentum matrices that define the geometric and dynamical periodic models are

$$\mathbf{Q}^{\mathrm{g}} := \mathrm{diag}(m), \quad m\big|_{-j}^{j} \Rightarrow \mathbf{P}^{\mathrm{g}} = \mathbf{\Phi}\mathbf{Q}^{\mathrm{g}}\mathbf{\Phi}^{-1}, \tag{7}$$

$$\frac{1}{2}(\mathbf{Q}^{\mathrm{d}})^2 = \mathrm{diag}(2\sin^2(\pi m/N)) \Leftarrow \frac{1}{2}(\mathbf{P}^{\mathrm{d}})^2 := -\frac{1}{2}\mathbf{\Delta}. \tag{8}$$

All the above matrices are real and symmetric, except for $\mathbf{P}^{\mathrm{g}}$, which is pure imaginary and skew-symmetric; thus, all are self-adjoint. Of course, neither pair commutes to the identity matrix of the Heisenberg algebra; and they are quite distinct, as we shall see below.

Out of Eqs. (7) and (8) we can construct two distinct generators of squeeze, obtained in the two ways of Eq. (4), but which are now different:

$$\mathbf{G}^{\mathrm{g}} := \frac{1}{2}(\mathbf{Q}^{\mathrm{g}}\mathbf{P}^{\mathrm{g}}+\mathbf{P}^{\mathrm{g}}\mathbf{Q}^{\mathrm{g}}), \tag{9}$$

$$\mathbf{G}^{\mathrm{d}} := -\mathrm{i}\left[\frac{1}{2}(\mathbf{Q}^{\mathrm{d}})^2,\frac{1}{2}(\mathbf{P}^{\mathrm{d}})^2\right], \tag{10}$$

where both generator matrices are pure-imaginary, skew-symmetric, and hence self-adjoint. Finally, the matrices that represent finite squeezing are the Lie exponentials of Eqs. (9) and (10),

$$\mathbf{S}^{\mathrm{g}}(\alpha^{\mathrm{g}}) := \exp(\mathrm{i}\alpha^{\mathrm{g}}\mathbf{G}^{\mathrm{g}}), \qquad \mathbf{S}^{\mathrm{d}}(\alpha^{\mathrm{d}}) := \exp(\mathrm{i}\alpha^{\mathrm{d}}\mathbf{G}^{\mathrm{d}}), \tag{11}$$

which are real, of unit determinant, orthogonal, and thus unitary; they form one-parameter groups belonging to $\mathsf{SO}(N)\subset\mathsf{SU}(N)\subset\mathsf{U}(N)$. These matrices act on the signal column vectors $\mathbf{f}=\|f_m\|$, so the squeeze of a real signal remains real, and the angles formed between different signal vectors are preserved under squeeze. The one-

parameter Lie groups are lines in the $\frac{1}{2}N(N-1)$-dimensional finite-volume subspace of SO($N$); when the eigenvalues of the squeezing generators are incommensurable, the lines are nonclosing Lissajous figures; this occurs in Eq. (9) when $N\geqslant 4$, and in Eq. (10) for odd $N\geqslant 5$ and even $N\geqslant 8$.

We underline that the square of Eq. (7) does *not* yield Eq. (8), and their scales turn out to be quite different. The spectum of positions of $\mathbf{Q}^{\mathrm{g}}$ in Eq. (7) is the unit-spaced, symmetric set $m\in[-j,j]$. On the other hand in Eq. (8), the position matrix $\mathbf{Q}^{\mathrm{d}}$ obtained as a diagonal square root has eigenvalues on the sine curve $2\sin(\pi m/N)$, ranging in $(-2,2)$; the spacing between them near $m=0$ is $\approx 2\pi/N$. To establish a scale factor between the squeezing parameters $\alpha^{\mathrm{g}}$ and $\alpha\equiv\alpha^{\mathrm{d}}$ in Eq. (11), we can compare either the spacing of the eigenvalues of position or their range—among other options. Since the same scale factor also relates momenta, the generators (9) and (10) may be expected to bear the square of that factor. The comparison of spacings leads to $\alpha^{\mathrm{g}}=(2\pi/N)^2\alpha$, while the comparison of ranges yields $\alpha^{\mathrm{g}}=(4/N)^2\alpha$. Moreover, we can also confront the actual spectra of the generator matrices (9) and (10); in both, the eigenvalues cluster into close pairs, and their ratios range between $\approx 1/N^2$ and $\approx 1/2N^2$. Although all these factors are of the same order of magnitude, there does not seem to be a unique argument to decide among them. We adopt the factor $(4/N)^2$ noting that in the figures below, the two renderings of squeezing appear reasonably similar. Also, since Eq. (8) is the matrix that was used in [2] to generate Fresnel transforms, we favor the parameter $\alpha\equiv\alpha^{\mathrm{d}}$ for easier compairson.

We further note that Eqs. (7) and (8) are not the only possible matrix pairs that one may propose to build squeezing generators. We can square the matrices (7), recognize the first as the generator of a Fresnel lens chirp, then use it and its Fourier transform as in Eq. (10) and call it a squeezing generator. Or, one can take the square root of Eq. (8) from the diagonal form and use it as in Eq. (9). Further, one may propose hybrid models where one foregoes the DFT as intertwiner between positions and momenta. Thus, beside the two definitions written above, for which we present the results of numerical experimentation, there are also a large variety of possible definitions for squeezing and magnification of finite signals. We choose again the sharp-edged rectangle function as our test signal, as we did in [2], because smooth, broad peaks comply too easily with expectations. And moreover, since the signals $\mathbf{f}=\|f_m\|$ reveal more of their true nature in phase space, we shall concurrently examine their Wigner function on the discrete torus $(m,k)$ [9], Eq. (50) [10],

$$W(\mathbf{f}|m,k) := \frac{1}{N}\sum_{n=-j}^{j} f^{*}_{m-n}\exp\left(\frac{4\pi \mathrm{i}}{N}kn\right)f_{m+n}. \qquad (12)$$

In Fig. 2 we show the rectangle signal $\mathrm{Rect}_{m_1,m_2}(m)$ (equal to 1 in $[m_1,m_2]$ and 0 outside) and its Wigner phase space representation by Eq. (12). The squeezings ($\alpha>0$) and magnifications ($\alpha<0$) of this signal under the "geometric" generator (9) are shown in Fig. 3, together with the corresponding Wigner functions. The action of

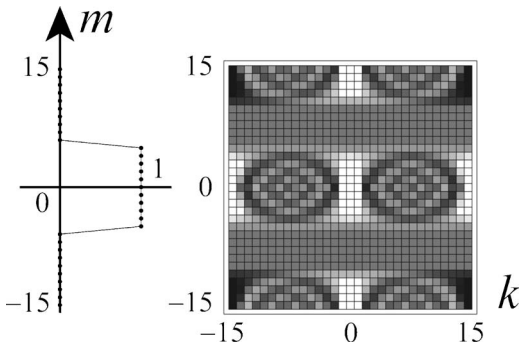


Fig. 2. Left, the discrete rectangle signal $\mathrm{Rect}_{-4,4}(m)$ on $N=31$ points ($j=15$). Right, the corresponding Wigner function on the discrete torus $(m,k)\in[-j,j]$ modulo $N$; the upper and lower boundaries represent the same meridian, as do the left and right boundaries; the basic pattern at the center (0,0) is (approximately) repeated at its three antipodes in the torus.

the "dynamical" generator (10) on the same signal appears in Fig. 4.

Signals in both Figs. 3 and 4 visibly squeeze for $\alpha>0$ and broaden for $\alpha<0$. The geometric version develops more but smaller oscillations than the dynamical version; in the latter, magnification emphasizes the discontinui-

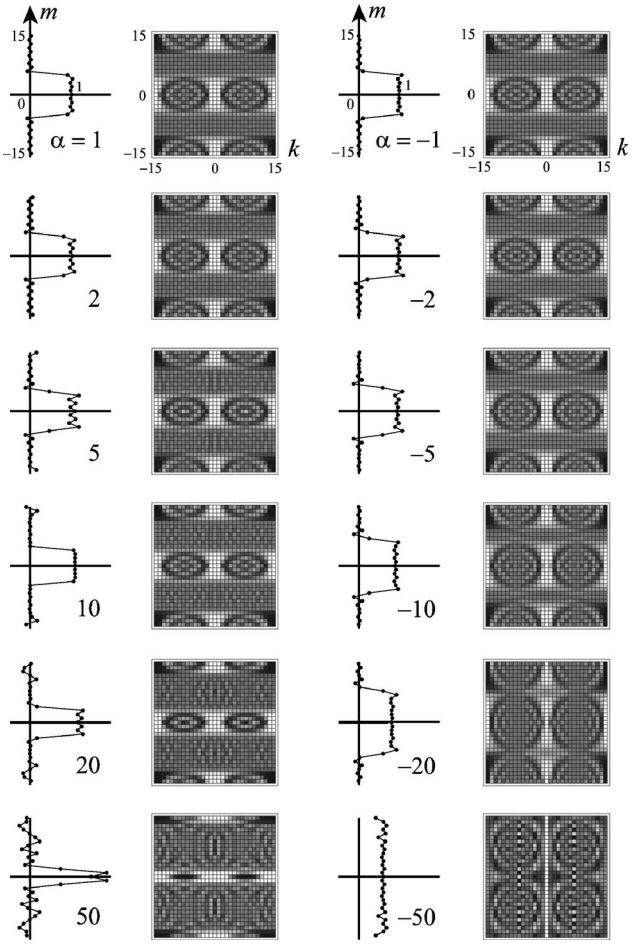


Fig. 3. Evolution of the discrete rectangle signal of the previous figure and the corresponding Wigner functions on the discrete torus, under the "geometric" version of squeezing and magnification (where position $\mathbf{Q}$ has a symmetric, equally spaced spectrum), with $\alpha^{\mathrm{g}}=(4/N)^2\alpha$ for the $\alpha$'s indicated between each pair.

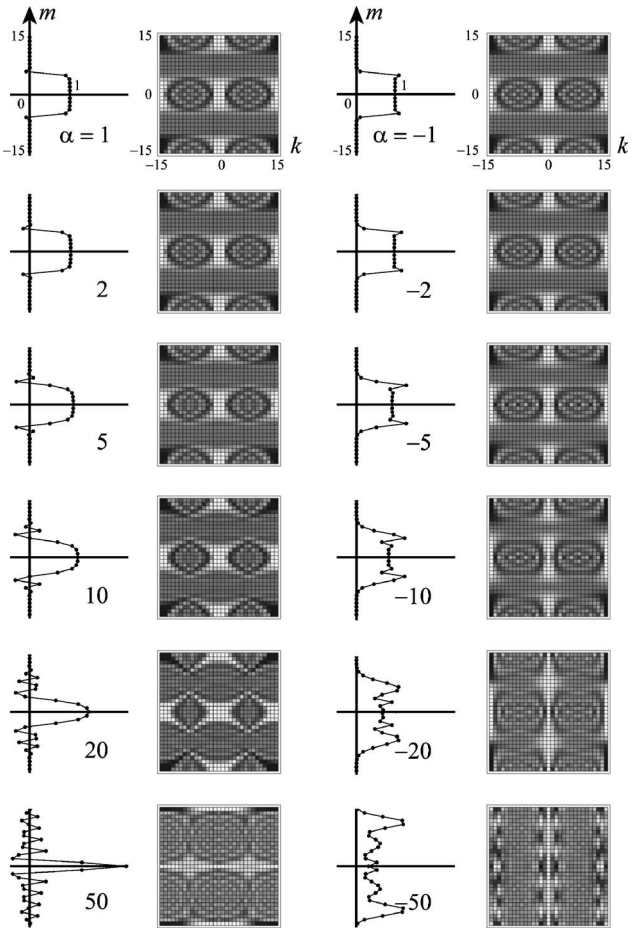


Fig. 4. Evolution of the rectangle signal and its Wigner function on the torus under the "dynamical" version of squeezing (based on momentum $\mathbf{P}^2=-\boldsymbol{\Delta}$), for the indicated values of $\alpha^{\mathrm{d}}\equiv\alpha$.

ties, while squeezing provides a rounder central peak. At the extreme values of $\alpha$, the signals would not be recognized as originating from a rectangle function by shape alone; here the Wigner function provides a complementary picture.

Several observations on the apparent symmetries of the Wigner function in the figures were made in [2] and need not be repeated here. We do note, however, that the Wigner functions exhibit four regions of squeeze, separated by the torus meridians $m,k\approx\pm\frac{1}{4}N$. In a neighborhood of the midpoints $(m,k)=(0,0)$, $(0,\pm\frac{1}{2}N)$, $(\pm\frac{1}{2}N,0)$, $(\pm\frac{1}{2}N,\pm\frac{1}{2}N)$, the peak and oscillations of the Wigner functions appear to flow in phase space consistently with the classical Fig. 1, although we have difficulty in defining the flows on the whole torus; these lines should appear as nested closed curves circulating inside each region. As one-parameter groups, squeezings are not periodic when the eigenvalues of Eqs. (9) and (10) are incommensurable, so the signal is never quite reconstituted. For larger $\alpha$'s, the Wigner functions in Figs. 3 and 4 become increasingly featureless. We have not searched for "revivals," but such events may be safely assumed to depend randomly on the dimension and the choice of squeezing generator to have eigenvalue pairs with near-to-simple ratios.

## 3. su(2) POSITION, MOMENTUM, AND ENERGY

We present now the su(2) oscillator model. In order not to repeat the full construction, which has been detailed in several previous papers [11–13], we recall only the essentials of the group-theoretical strategy we follow here to understand $N$-point finite, nonperiodic Hamiltonian systems. Signals are complex $N$-vectors that specify the state of the system (as in quantum mechanics) and evolve subject to unitary $N\times N$ matrices ($N=2j+1$). Signals are thus handled as states (or wavefunctions) of spin $j$ (integer or half-integer), whose "rigid" SU(2) rotations include the impression of a chirp phase on the signal, and the fractional Fourier (–Kravchuk) transform, which bridges between the position and momentum/wavenumber representations (below).

The asignments between the observables of the system and the generators of the ("old" angular momentum) algebra su(2) are postulated to be as follows:

$$\text{position:}\qquad \mathcal{Q}=\mathcal{L}_1, \tag{13}$$

$$\text{momentum:}\qquad \mathcal{P}=\mathcal{L}_2. \tag{14}$$

$$\text{(displaced) energy:}\qquad \mathcal{H}=\mathcal{L}_3+\left(j+\frac{1}{2}\right)1. \tag{15}$$

Thus, the "new" su(2) commutation relations are

$$[\mathcal{H},\mathcal{Q}]=\mathrm{i}\mathcal{P},\qquad [\mathcal{P},\mathcal{H}]=\mathrm{i}\mathcal{Q},$$

$$[\mathcal{Q},\mathcal{P}]=\mathrm{i}\left[\mathcal{H}-\left(j+\frac{1}{2}\right)1\right]. \tag{16}$$

The first two are the geometric and dynamic Hamilton equations, respectively, for the oscillator, while the third is the algebraic postulate that is specific for the su(2) finite-oscillator model.

Commonly known results from quantum angular momentum can be applied straightforwardly to state some properties of this model. In the space of $N$-point signals, these operators of position, momentum, and (displaced) energy have spectra that are intrinsically discrete, finite, and equally spaced: $\{-j,-j+1,\ldots,j\}$. Also useful for our purposes is the *number* operator, defined as

$$\text{number: }\mathcal{N}:=\mathcal{H}-\frac{1}{2}1=\mathcal{L}_3+j1. \tag{17}$$

whose spectrum is $\nu\in\{0,1,2,\ldots,2j\}$.

Using the Dirac bracket notation, a finite $N$-point signal $\mathbf{f}$ is represented by its coordinates in the position eigenbasis, $\{f_m\}_{m=-j}^{j}$, $f_m:={}_1\langle j,m|\mathbf{f}\rangle$. Similarly, its momentum coordinates are $\tilde{f}_k:={}_2\langle j,k|\mathbf{f}\rangle$, and its (number, energy) content along the 3-axis is $\hat{f}_\mu:={}_3\langle j,\mu|\mathbf{f}\rangle$. The wave functions of the finite oscillator are the overlaps between the position and energy bases, $|j,m\rangle_1$ and $|j,\nu-j\rangle_3$; they are given in terms of the well-known Wigner "little"-$d$ rotation functions [14], Sect. 3.6,

$$\psi_\nu^{(j)}(m) := {}_1\langle j,m|j,\nu-j\rangle_3 = d^j_{m,\nu-j}\left(-\frac{1}{2}\pi\right) = d^j_{\nu-j,m}\left(\frac{1}{2}\pi\right), \tag{18}$$

numbered by $\nu\in[0,2j]$. Since these functions may be written in terms of Kravchuk polynomials of degree $\nu$ in position $m$ (times the square root of a binomial distribution in $m$) [11,15], we have appended the name of Kravchuk to several functions and operators that appear in the su(2) model to distinguish them from their continuous counterparts.

In orthonormal bases, the operators (13)–(15) are represented by self-adjoint (Hermitian) $N\times N$ matrices. In the commonly used basis $|j,\mu\rangle_3$, $\mathcal{N}$ is represented by diag$(0,1,\ldots,N-1)$; in the su(2) model; however, signals are understood to be in the eigenbasis of position, namely, $|j,m\rangle_1$, where the matrix representatives of Eqs. (13), (14), and (17), have elements

$$Q_{m,m'} := m\,\delta_{m,m'}, \qquad m,m'\in[-j,j], \tag{19}$$

$$P_{m,m'} := -\mathrm{i}\left(\frac{1}{2}\sqrt{(j-m)(j+m+1)}\,\delta_{m+1,m'} - \frac{1}{2}\sqrt{(j+m)(j-m+1)}\,\delta_{m-1,m'}\right), \tag{20}$$

$$N_{m,m'}+j\delta_{m,m'} := \frac{1}{2}\sqrt{(j-m)(j+m+1)}\,\delta_{m+1,m'} + \frac{1}{2}\sqrt{(j+m)(j-m+1)}\,\delta_{m-1,m'}. \tag{21}$$

In particular, in Eq. (20) we see that the matrix analog of momentum, $\mathbf{P}=\|P_{m,m'}\|$, acting on a signal $\mathbf{f}=\|f_m\|$, yields $-\mathrm{i}$ times its central derivative, $f'_m := \frac{1}{2}(c^+_m f_{m+1} - c^-_m f_{m-1})$, but with unequal positive coefficients $c^\pm_m = [(j-m)(j+m+1)]^{1/2}$. There is no ambiguity at the ends of the interval because $f'_{\mp j} = \pm\frac{1}{2}(2j)^{1/2} f_{\mp j\pm 1}$.

In the su(2) model, the fractional Fourier integral and Fresnel transforms of continuous systems have their finite counterpart in the one-parameter groups [1,2],

$$\text{Fourier–Kravchuk:} \qquad \mathcal{K}^{(\kappa)} := \exp\left(-\mathrm{i}\frac{1}{2}\pi\kappa\mathcal{N}\right), \tag{22}$$

$$\text{Fresnel–Kravchuk:} \qquad \mathcal{F}(z) := \exp\left(\mathrm{i}\frac{1}{2}z\mathcal{P}^2\right). \tag{23}$$

The Fourier–Kravchuk transforms (22) are rotations around the 3-axis and are elements of the group SU(2) of rigid rotations of a sphere; the Fresnel–Kravchuk transforms, on the other hand, are the exponentials of a *quadratic* element of su(2) and finite analog of second-degree *aberrations* of the phase space of signals. Each transform is represented by $N\times N$ unitary matrices whose elements are given again in terms of the Wigner little-$d$ functions [1], Eq. (40), and [2], Eq. (34).

In this paper we propose to build the generator of squeezings and magnifications in finite systems using the symmetrized quadratic operators (5), but with the su(2) assignments (13)–(15), in their $N\times N$ matrix representation,

$$\mathcal{G} := \{\mathcal{Q}\mathcal{P}\}_{\mathrm{W}} = (\mathcal{L}_1\mathcal{L}_2 + \mathcal{L}_2\mathcal{L}_1),$$

$$\mathbf{G} = \frac{1}{2}(\mathbf{QP}+\mathbf{PQ}). \tag{24}$$

The matrix elements of this squeezing generator are found from Eqs. (19) and (20),

$$G_{m,m'} = -\mathrm{i}\left(\left(m+\frac{1}{2}\right)\sqrt{(j-m)(j+m+1)}\,\delta_{m+1,m'} - \left(m-\frac{1}{2}\right)\sqrt{(j+m)(j-m+1)}\,\delta_{m-1,m'}\right). \tag{25}$$

This representation is bidiagonal, pure imaginary, skew-symmetric, and self-adjoint, its trace is null, and its eigenvalues are incommensurable for odd $N\geqslant 5$ ($j\geqslant 2$) and even $N\geqslant 8$ ($j\geqslant 7/2$).

And now, as in Eq. (11), the finite squeezing operators and matrices are the Lie exponentials

$$\mathcal{S}(a) := \exp(\mathrm{i}a\mathcal{G}), \qquad \mathbf{S}(a) := \exp(\mathrm{i}a\mathbf{G}). \tag{26}$$

These matrices are real, orthogonal, hence unitary, and of unit determinant; again, the set $a\in\mathsf{R}$ forms a one-parameter group line within the group $\mathsf{SO}(N)\subset\mathsf{SU}(N)\subset\mathsf{U}(N)$; the lines draw nonclosing Lissajous figures when the eigenvalues of Eq. (25) are incommensurable. For our purposes here it was sufficient to handle the matrices (26) for the given $N$ by numerical computation, since the exponential of Eq. (25) does not seem reducible to a simple analytic expression.

The finite analog of Eq. (6), namely, $[\frac{1}{2}\mathcal{L}_1^2, \frac{1}{2}\mathcal{L}_2^2]$, gives a second option to define su(2) squeezing; we do not address it here for reasons that will be discussed in the Conclusions.

## 4. WIGNER FUNCTION ON THE PHASE SPACE SPHERE

The su(2) model for finite systems entails a semiclassical picture of phase space, where it is expanded into three dimensions—one for each of its three generators $\mathcal{L}_1,\mathcal{L}_2,\mathcal{L}_3$. This we have called *meta*-phase space; its Cartesian coordinates are position, momentum, and (displaced) energy, $\vec{v}=(q,p,\mu)\in\mathsf{R}^3$. The concept was introduced in [13] for su(2) and generalized in [16] for essentially arbitrary finite-dimensional Lie algebras.

The construction of meta-phase space hinges on defining an $\mathsf{R}^3$ manifold $\vec{v}$ of Wigner operators (elements of the SU(2) group ring),

$$\mathcal{W}(\vec{v}) := \int_{\mathsf{su}(2)} \mathrm{d}g(\vec{w})\exp\mathrm{i}[w_1(q-\mathcal{Q}) + w_2(p-\mathcal{P}) + w_3(\mu-\mathcal{L}_3)], \tag{27}$$

where the integration is over the group manifold $g(\vec{w})\in\mathsf{SU}(2)\overset{2:1}{=}\mathsf{SO}(3)$ (a 3-sphere $\mathsf{S}^3$). For integer $j$ (odd $N$) we

reduce this integral to the manifold of rotations given by the rotation axis $\hat{u}(\theta,\phi)$ and angle $\psi$, as

$$\vec{w} := \psi\hat{u}(\theta,\phi) = \begin{pmatrix} w_1 \\ w_2 \\ w_3 \end{pmatrix} = \begin{pmatrix} \psi\sin\theta\sin\phi \\ \psi\sin\theta\cos\phi \\ \psi\cos\theta \end{pmatrix}, \quad \begin{matrix} 0 \leqslant \psi < 2\pi, \\ 0 \leqslant \theta \leqslant \pi, \\ 0 \leqslant \phi < 2\pi. \end{matrix} \tag{28}$$

In these coordinates, the invariant Haar measure $\mathrm{d}g(\vec{w})$ in Eq. (27) is [17, Sect. 3.V], [13],

$$\mathrm{d}g(\psi,\theta,\phi) = \frac{1}{2}\sin^2\frac{1}{2}\psi\sin\theta\,\mathrm{d}\psi\mathrm{d}\theta\mathrm{d}\phi. \tag{29}$$

At this time we can also introduce the marginal operator of position,

$$\mathcal{M}_{\mathcal{Q}}(q) = \int_{\mathsf{R}}\mathrm{d}p\int_{\mathsf{R}}\mathrm{d}\mu\,\mathcal{W}(q,p,\mu) = (2\pi)^2\int_{-\pi}^{\pi}\mathrm{d}w\,\exp[\mathrm{i}w(q-\mathcal{Q})]. \tag{30}$$

The Wigner function in meta-phase space of a $(2j+1)$-point signal $\mathbf{f}=\|f_m\|$ is naturally defined as the expectation value of the manifold of Wigner operators in that state,

$$W(\mathbf{f}|q,p,\mu) := \langle\mathbf{f}|\mathcal{W}(q,p,\mu)|\mathbf{f}\rangle = \sum_{m,m'} f_m^* W^{(j)}_{m,m'}(q,p,\mu) f_{m'}. \tag{31}$$

There exist analytic expressions for the matrix elements $W^{(j)}_{m,m'}(q,p,\mu)$—see [13,16,2], Eqs. (38)–(40).

As a check, information about the finite signal $\mathbf{f}$ can be recovered from its su(2) Wigner function (31) over $\mathsf{R}^3$, through projection on the position axis. This is the marginal of position,

$$M(\mathbf{f}|q) := \int_{\mathsf{R}}\mathrm{d}p\int_{\mathsf{R}}\mathrm{d}\mu\,W(\mathbf{f}|q,p,\mu) = \langle\mathbf{f}|\mathcal{M}_{\mathcal{Q}}(q)|\mathbf{f}\rangle = (2\pi)^3\sum_m |f_m|^2\,\mathrm{sinc}\,\pi(q-m). \tag{32}$$

Because of the sinc factor, when $q$ is an integer $m\in[-j,j]$, $M(\mathbf{f}|m)=(2\pi)^3|f_m|^2$ returns the absolute value of the signal at that point. Elsewhere, we have a finite, smooth sinc interpolation in position. Similar marginals can be written to recover the momentum or energy contents of a finite signal.

Other marginals of the su(2) Wigner function on meta-phase space $\vec{v}\in\mathsf{R}^3$ are also relevant. The integration over all angles of the sphere yields a marginal function of the radial coordinate $|\vec{v}|=r\in\mathsf{R}^+$. When we recall that in the $(2j+1)$-dimensional representation $j$, the invariant Casimir operator of the algebra is a constant,

$$\mathcal{Q}^2+\mathcal{P}^2+\mathcal{L}_3^2 = j(j+1)\mathit{1}, \tag{33}$$

we see that this radial marginal will be independent of $\mathbf{f}$, and a function of $r$ only. This marginal is also the trace of the matrix $W^{(j)}_{m,m'}(q,p,\mu)$ in Eq. (31) and can be computed as an analytic expression; it is strongly peaked in $j<r<j+1$ [13]. For this reason, in [13,18,2] we chose to "slice" meta-phase space at the radius $r=j+\frac{1}{2}$ near the maximum of Eq. (33), noting that the plotted results are quite independent of the exact radius chosen. Here we use this value to plot—on a plane—the Wigner functions that live in $\mathsf{R}^3$, as shown in Fig. 5. The angular marginal that is obtained integrating the su(2) Wigner function over the radius $r\in\mathsf{R}^+$ yields the Stratonovich–Agarwal Wigner function [19,20] over the sphere, as was shown in [21]. Corresponding to Fig. 2 on the torus, in Fig. 6 we show the su(2) Wigner function of the same rectangle signal of Fig. 2, and also in [2], Fig. 9, where some key numerical values are given for the peak and for the very small negative dimples.

A classical meta-phase space $(q,p,\mu)$ on the sphere $q^2+p^2+\mu^2=(j+\frac{1}{2})^2$, or other conics, can be formulated using Berezin brackets [22], Chap. 7. These behave as Poisson brackets but in *three* variables: $\{q,p\}_{\mathrm{B}}=\mu$, $\{\mu,q\}_{\mathrm{B}}=p$, and $\{p,\mu\}_{\mathrm{B}}=q$, with the usual distribution under sum and multiplication of first derivatives. A transformation generated by a function $g(q,p)$ through $\exp(\alpha\{g,\circ\}_{\mathrm{B}})$, will preserve the sphere and the lines $g(q,p)=$constant. In particular, the generator of squeezings, $g_{\mathrm{S}}(q,p)=qp$ will generate lines of flux along the intersections of the hyperbolic cylinders $qp=$constant and the sphere, as shown in Fig. 5. In the vicinity of the bottom pole $(q,p,-j-\frac{1}{2})$, these flux lines match those of squeeze in the flat phase space of Fig. 1.

We proceed thus to exponentiate the matrix $\mathbf{G}$ in Eq. (24) to generate finite squeezing and magnification, $\mathbf{S}(a)$ in Eq. (26), for $a>0$ and $a<0$. These matrices were applied directly to the signal vector $\mathbf{f}$ through multiplication. As previously, we chose the rectangle test signal $\mathrm{Rect}_{m_1,m_2}(m)$ with the same parameters as in Figs. 3 and 4, to display its su(2) squeezing in Fig. 7. There appear the signals and their phase space representations on the sphere, flattened out to its colatitude and azimuth coordinates $(\beta,\gamma)$ referred to the position axis, as indicated in

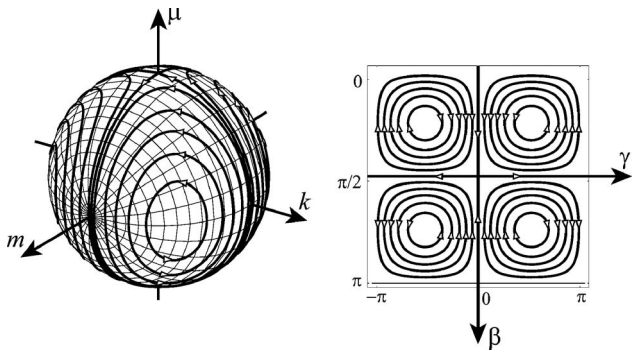


Fig. 5. Left, the su(2) Wigner function lives in the meta-phase space $(m,k,\mu)\in\mathsf{R}^3$ of position, momentum, and (displaced) energy. Spherical coordinates $(\beta,\gamma)$ are referred to the position axis $(m)$. The thick arrowed lines represent the global flux due to squeezing (explained in the text). Right, the $(\beta,\gamma)$ plane presents the su(2) Wigner function for easier comparison with the previous figures (on the discrete torus). The origin of coordinates coincides with the "bottom pole" of ground energy at $(\beta=\frac{1}{2}\pi,\gamma=0)$; the "top pole" is at $(\beta=\frac{1}{2}\pi,\gamma=\pm\pi)$; the points on the momentum axis are $(\frac{1}{2}\pi,\pm\frac{1}{2}\pi)$. The flux lines under squeezing are indicated by the thick arrowed lines (cf. Fig. 1).

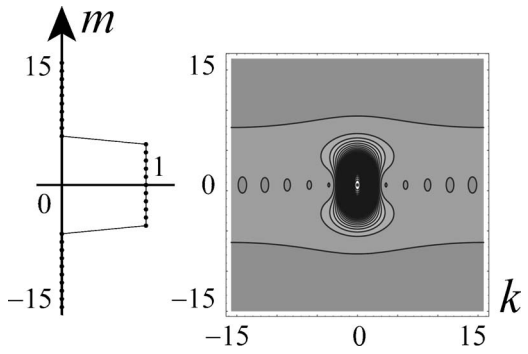


Fig. 6. Left, the rectangle function $\mathrm{Rect}_{-5,5}(m)$ as an $N=31$-point signal. Right, the corresponding su(2) Wigner function on the sphere, displayed by its level curves on a square. The vertical and horizontal axes are labeled by $(m,k)$ for direct comparison with Fig. 2; this square is actually the $(\beta,\gamma)$ plane of the sphere, as explained in Fig. 5. The Wigner function has a strong peak centered at the origin and elongated over the width of the signal, with shallow dimples of negative values. We display 40 level curves to emphasize the behavior of the su(2) Wigner function where its values are small or negative.

Fig. 5. Again, we are faced with the problem of establishing a scale factor between the parameter $a$ in Eq. (26) and the parameters $\alpha^{\mathrm{g}}=(4/N)^2\alpha$ and $\alpha\equiv\alpha^{\mathrm{d}}$ in Eq. (11). We had expected $a=\alpha^{\mathrm{g}}$ because the eigenvalue ranges of $\mathbf{Q}^{\mathrm{g}}$ in Eq. (7) and of $\mathbf{Q}$ in Eq. (19) are the same (although the range of $\mathbf{G}^{\mathrm{g}}$ eigenvalues exceeds that of $\mathbf{G}$ by some 37%). Finally, we had to resort to direct comparison of the figures to propose $a=\frac{1}{5}(4/N)^2\alpha$ and keep the issue of scaling for further understanding.

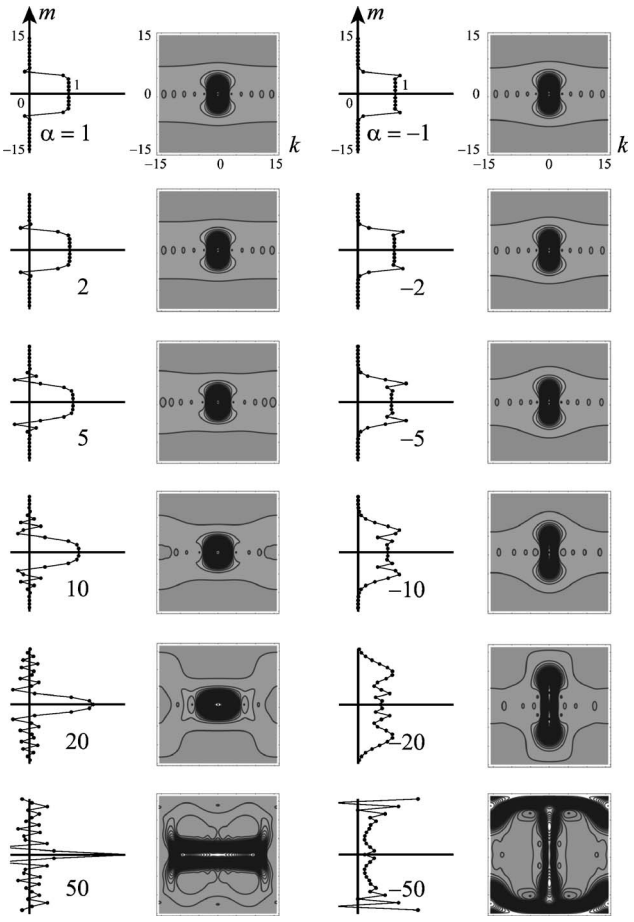


Fig. 7. Evolution of the rectange signal and its Wigner function on the sphere (as explained in Fig. 6), under su(2) squeezing of positions by the factors $e^{-a}$, with $a=\frac{1}{5}(4/N)^2\alpha$, for the indicated values of $\alpha$ (cf. Figs. 3 and 4).

In the su(2) model, as evinced by Fig. 7, squeezing $a>0$ compresses the peak of the Wigner function along the bottom meridian between the two position poles, $(0\leqslant\beta\leqslant\pi,\ \gamma=0)$, and stretches it along the equator between the two momentum poles, $(\beta=0,\ -\pi<\gamma\leqslant\pi)$, and vice versa under magnification $a<0$, in accordance with the flow lines on the classical sphere of Fig. 5. We note that in the Wigner function of Fig. 7, the peak mantains its integrity rather well, while in the rest of the picture the Wigner function is carried along the flow lines, necessarily wiggling somewhat [23] due to the nonlinear transformations of the classical underlying phase space. A semiclassical approximation to finite squeeze would consist of ignoring these wiggles. Finally, the movement of the very small negative dimples of the su(2) Wigner function is interesting; it can be compared with their behavior under the Fresnel–Kravchuk transform in [2], Fig. 9.

## 5. CONCLUSIONS

We have classical, wave, and finite versions of squeezing, generated by $g_{\mathrm{S}}=qp$ on signals, states, or wavefunctions of finite systems. We worked with two distinct phase space representations for finite systems: the discrete torus and the sphere. On the torus, we examined two versions of squeezing for periodic systems, according to geometric or dynamical desiderata (linear or sine-spaced eigenvalues, vibrating ring lattices, Fresnel lenses); clearly, other choices can be proposed that will yield squeezings and magnifications different from those in Figs. 3 and 4. This ambiguity is an advantage when the choice tailors a given physical model, but it opens questions on mathematical consistency. On the sphere, the su(2) model for finite Hamiltonian systems inherits the mathematical corpus of group theory and its elegant account of manifest and hidden symmetries.

We proposed a generator of su(2) squeezings, $\mathcal{G}$ in Eq. (24); at the end of that section we remarked that a second choice exists: that which instead of Eq. (5) follows the classical bracket (6) between the Fresnel and chirp generators. Translating this to commutators between su(2) generators, respecting order and the Leibnitz rule, one obtains

$$\mathcal{G}' := \left[\frac{1}{2}\mathcal{L}_1^2,\frac{1}{2}\mathcal{L}_2^2\right]=\mathrm{i}\frac{1}{2}(\mathcal{L}_1\mathcal{L}_2\mathcal{L}_3+\mathcal{L}_3\mathcal{L}_2\mathcal{L}_1), \tag{34}$$

among several other equivalent orderings of the three operators. This differs from Eq. (24) in that it contains an extra factor $\mathcal{L}_3$. Its corresponding classical function in meta-phase space is $g'_{\mathrm{S}}=qp\mu$, which generates a flux of closed loops on the sphere divided into octants, instead of the quadrants shown in Fig. 5. The two flows coincide at the bottom pole, and are opposite at the top pole; and both limit to the classical squeeze in Fig. 1 when $N\to\infty$, as su(2) contracts to the Heisenberg–Weyl algebra [24]. Extra factors or polynomials of $\mathcal{L}_3$ will have the similar ef-

fect of segmenting the vertical flow of phase space on the sphere; in this regard, our choice to define the squeezing generator $\mathcal{G}$ through Eq. (24) is the most economical. Finally, as stated in Section 1, with Fourier, Fresnel, and squeezing, we have finite counterparts of the full group $\mathsf{Sp}(2,\mathsf{R})$ of linear canonical transformations.

The classification of aberrations and other issues should be resolved as we proceed to understand the $\mathsf{U}(N)$ group of transformations of $N$-point signals in terms of rigid transformations and aberrations generated by ordered products of $\mathsf{su}(2)$ elements, mirroring their structure in geometric optics [22], Part 4—but finite, because $\mathsf{U}(N)$ admits of no more than $N^2$ independent transformations. This problem is open on the torus but is well posed on the sphere.

## ACKNOWLEDGMENTS

We thank L. E. Vicent (Facultad de Ciencias, Universidad Autónoma del Estado de Morelos) for discussions on the subjects of this paper. Support from the SEP–CONACYT project 44845 and DGAPA–UNAM project IN102603, *Óptica Matemática* are gratefully acknowledged.

## REFERENCES

1. K. B. Wolf and G. Krötzsch, "Geometry and dynamics in the fractional discrete Fourier transform," J. Opt. Soc. Am. A **24**, 651–658 (2007).
2. K. B. Wolf and G. Krötzsch, "Geometry and dynamics in the Fresnel transform in finite systems," J. Opt. Soc. Am. A **24**, 2568–2577 (2007).
3. M. Moshinsky and C. Quesne, "Linear canonical transformations and their unitary representation," J. Math. Phys. **12**, 1772–1780 (1971).
4. K. B. Wolf, *Integral Transforms in Science and Engineering* (Plenum, 1979).
5. I. D. Ado, "The representation of Lie algebras by matrices," Trends Am. Math. Soc. **9**, 308–327 (1962).
6. E. P. Wigner, "On the quantum correction for thermodynamic equilibrium," Phys. Rev. **40**, 749–759 (1932).
7. M. Hillery, R. F. O'Connel, M. O. Scully, and E. P. Wigner, "Distribution functions in physics: fundamentals," Phys. Rep. **259**, 121–167 (1984).
8. H.-W. Lee, "Theory and applications of the quantum phase-space distribution functions," Phys. Rep. **259**, 147–211 (1995).
9. U. Leonhardt, "Discrete Wigner function and quantum-state tomography," Phys. Rev. A **53**, 2998–3013 (1996).
10. W. K. Wooters, "A Wigner-function formulation of finite-state quantum mechanics," Ann. Phys. (N.Y.) **176**, 1–21 (1987).
11. N. M. Atakishiyev and K. B. Wolf, "Fractional Fourier–Kravchuk transform," J. Opt. Soc. Am. A **14**, 1467–1477 (1997).
12. N. M. Atakishiyev, G. S. Pogosyan, and K. B. Wolf, "Finite models of the oscillator," Phys. Part. Nucl. **36**, 521–555 (2005).
13. N. M. Atakishiyev, S. M. Chumakov, and K. B. Wolf, "Wigner distribution function for finite systems," J. Math. Phys. **39**, 6247–6261 (1998).
14. L. C. Biedenharn and J. D. Louck, *Angular Momentum in Quantum Physics*, Encyclopedia of Mathematics and Its Applications, G.-C. Rota, ed. (Addison-Wesley, 1981).
15. A. F. Nikiforov, S. K. Suslov, and V. B. Uvarov, *Classical Orthogonal Polynomials of a Discrete Variable* (Springer-Verlag, 1991).
16. S. T. Ali, N. M. Atakishiyev, S. M. Chumakov, and K. B. Wolf, "The Wigner function for general Lie groups and the wavelet transform," Ann. Inst. Henri Poincare **1**, 685–714 (2000).
17. R. Gilmore, *Lie Groups, Lie Algebras, and Some of their Applications* (Wiley Interscience, New York, 1978).
18. S. M. Chumakov, A. Frank, and K. B. Wolf, "Finite Kerr medium: macroscopic quantum superposition states and Wigner functions on the sphere," Phys. Rev. A **60**, 1817–1823 (1999).
19. R. L. Stratonovich, "On distributions in representation space," JETP **31**, 1012–1020 (1956) [Sov. Phys. JETP **4**, 891–898 (1957)].
20. G. S. Agarwal, "Relation between atomic coherent-state representation, state multipoles, and generalized phase-space distributions," Phys. Rev. A **24**, 2889–2896 (1981).
21. S. M. Chumakov, A. B. Klimov, and K. B. Wolf, "On the connection of two Wigner functions for spin systems," Phys. Rev. A **61**, 034101(3), (2000).
22. K. B. Wolf, *Geometric Optics on Phase Space* (Springer-Verlag, 2004).
23. A. L. Rivera, N. M. Atakishiyev, S. M. Chumakov, and K. B. Wolf, "Evolution under polynomial Hamiltonians in quantum and optical phase spaces," Phys. Rev. A **55**, 876–889 (1997).
24. N. M. Atakishiyev, G. S. Pogosyan, and K. B. Wolf, "Contraction of the finite one-dimensional oscillator," Int. J. Mod. Phys. A **18**, 317–327 (2003).